

Impact dynamics near unilaterally constrained grazing orbits

Stéphane Junca^{*}, Huong Le Thi^{*}, Mathias Legrand^{**}, and Anders Thorin^{**}

^{*}*Mathematical Laboratory JAD, Université Côte d'Azur, Inria, CNRS, Nice, France,*

^{**}*Department of Mechanical Engineering, McGill University, Montréal, Québec, Canada*

Summary. The dynamics of vibro-impact systems near grazing is known to be singular. The authors have recently exhibited nonlinear modal motions in the vicinity of grazing orbits within a conservative framework, suggesting the latter play an important role in the dynamics. In this work, insights on the dynamics of solutions near some periodic grazing orbits are given. It is found that the first return time may involve a square-root singularity or a cube-root singularity and also become discontinuous. These properties may affect the first return map and thus the dynamics near grazing orbits.

Motivation

In vibration analysis of unilaterally constrained systems, a grazing contact is a contact with zero-velocity. In contrast to the smooth dynamics framework, the dynamics of vibro-impact mechanical systems is singular near grazing orbits, involving square-root singularities of the first return time [10]. As experienced by the authors, periodic grazing orbits (i.e. linear modes) are often the starting points to nonlinear modes of vibration [9, 12, 14], defined as continuous one-parameter families of periodic orbits [6, 15] of nonlinear systems. The aim of this work is to explore such dynamics in the neighborhood of a linear grazing modal motion (LGM) and in the neighborhood of a periodic solution with a sticking phase (SPP).

Model

As illustrated in Figure 1, consider a conservative N -degree-of-freedom (dof) oscillator consisting of a chain of N masses m_j , $j = 1, \dots, N$ connected by N springs, one of which being attached to the ground. The system is also unilaterally constrained by a rigid foundation. The i th spring acts on the j th mass via the stiffness k_{ij} . The displacement

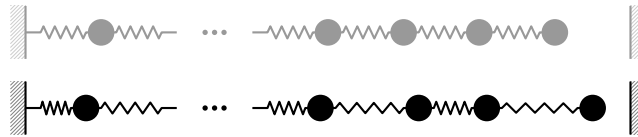


Figure 1: A unilaterally constrained N -spring-mass system: at equilibrium [gray] and in its current configuration [black].

of the masses with respect to their equilibrium position is denoted by u_j and the corresponding velocities and accelerations are denoted by \dot{u}_j and \ddot{u}_j , respectively. The distance between the constraint and the equilibrium position of the unilaterally constrained mass is d . The dynamics is governed by the following equations:

$$\begin{cases} \mathbf{M}\ddot{\mathbf{u}} + \mathbf{K}\mathbf{u} = \mathbf{r} & (1a) \\ \mathbf{u}(0) = \mathbf{u}_0, \quad \dot{\mathbf{u}}(0) = \dot{\mathbf{u}}_0 & (1b) \\ u_N(t) \leq d, \quad R(t) \leq 0, \quad (u_N(t) - d)R(t) = 0, \quad \forall t & (1c) \\ \dot{\mathbf{u}}(t)^\top \mathbf{M}\dot{\mathbf{u}}(t) + \mathbf{u}(t)^\top \mathbf{K}\mathbf{u}(t) = \mathbf{E}(\mathbf{u}(t)) = \mathbf{E}(\mathbf{u}(0)), & (1d) \end{cases}$$

where $\mathbf{M} = \text{diag}(m_j)_{1 \leq j \leq N}$, $\mathbf{K} = (k_{ij})_{1 \leq i, j \leq N}$, $\mathbf{u}(t) = (u_j(t))_{1 \leq j \leq N}$, and $\mathbf{r}(t) = (0, \dots, 0, R(t))$. The term $R(t)$ captures the reaction force acting on the last mass and induced by the constraint. The last equation ensures that the total energy \mathbf{E} of the system is preserved. System (1) without (1d) is not well posed: it is known that uniqueness is not guaranteed for the initial value problem [1, 11]. This is usually overcome by incorporating an impact law into the formulation. Here, since we are interested in non-dissipative dynamics, condition (1d) is enforced: the total energy is preserved during the motion. This implies the existence of a perfectly elastic impact law of the form $\dot{u}_N^+ = -e\dot{u}_N^-$ with $e = 1$ where \dot{u}_N^- and \dot{u}_N^+ respectively stand for the pre- and post-impact velocities of mass N . The impact law with $e = 1$ is equivalent to the conservation of the total energy.

First return time and square-root singularity

Without loss of generality, the initial data is such that the last mass lies on the wall: $u_N(0) = d$. The first return time (FRT) is defined as the duration between two successive contacts; a precise definition follows. This governs the choice of the Poincaré section as the hyperplane $\mathcal{H} = \{[\mathbf{u}, \dot{\mathbf{u}}]^\top \in \mathbb{R}^{2N}, u_N = d\}$ of the phase-space [4], on which is defined the Poincaré Map. Two questions on the first return time naturally arise:

1. Does it exist? In other words, does the last mass always return to the wall? Generically, the answer is affirmative.

2. Is the first return time a smooth function of the initial data? The answer is also affirmative in the case of impact with nonzero velocity [2].

This property however no longer holds for grazing orbits. It is not impossible that the last mass grazes with the wall once but then never comes back.

On the other extreme, could there be a solution with a sticking phase of infinite duration for which the first return time does not exist? When the first return time does exist, it is never smooth in term of initial data because of the presence of the square-root singularity [2, 10]. Indeed, it is already singular for a one-dof oscillator [5]. This square-root singularity is investigated in details within the simple mathematical framework of system (1) in [8], based on the implicit function theorem adapted to this degenerate contact. The impact hyperplane \mathcal{H} is of dimension $2N - 1$. It is divided into three

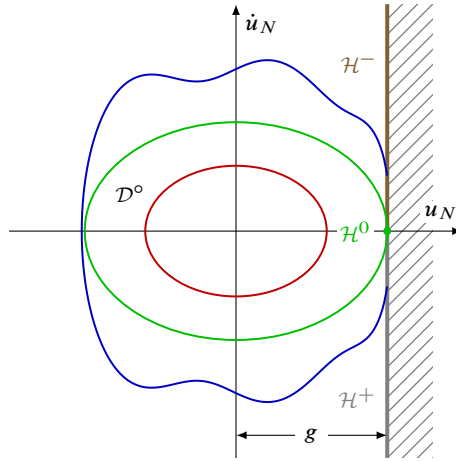


Figure 2: Cross-section of the admissible state-space.

disjoint subsets as depicted in Figure 2:

$$\begin{aligned}\mathcal{H}^- &= \{[\mathbf{u}, \dot{\mathbf{u}}^-]^\top \in \mathbb{R}^{2N}, u_N = d \text{ and } \dot{u}_N^- > 0\} \\ \mathcal{H}^+ &= \{[\mathbf{u}, \dot{\mathbf{u}}^+]^\top \in \mathbb{R}^{2N}, u_N = d \text{ and } \dot{u}_N^+ < 0\} \\ \mathcal{H}^0 &= \{[\mathbf{u}, \dot{\mathbf{u}}]^\top \in \mathbb{R}^{2N}, u_N = d \text{ and } \dot{u}_N = 0\}\end{aligned}$$

By conservation of energy, it can be seen that the solution involving a contact with non-zero velocity will always experience a later contact. The problem of whether there will be a subsequent contact or not emerges only on \mathcal{H}^0 . It is proven [8] that most orbits which belong to \mathcal{H}^0 feature an infinite number of closing contacts. The set of these orbits is denoted by \mathcal{H}_∞^0 ¹. As a consequence, the Poincaré section defined below is reasonable and the first return time is then shown to be well defined.

Definition 1 (Poincaré section) *The Poincaré section $\mathcal{H}_P \subset \mathcal{H}$ is the union of the set of initial data with non-zero velocity contacts and the set of initial data with zero velocity contact that gives rise to an infinite number of subsequent closing contacts:*

$$\mathcal{H}_P = \mathcal{H}^- \cup \mathcal{H}_\infty^0. \quad (2)$$

Definition 2 (First return time) *Let \mathbf{u} be a solution to (1) with the initial data $\mathbf{W} \in \mathcal{H}_P$ at the initial time $t = 0$, i.e. $u_N(0) = \mathbf{e}_N^\top \mathbf{u}(0) = d$. The first return time $T = T(\mathbf{W}) > 0$ is defined by*

$$T(\mathbf{W}) = \min\{t > 0 : u_N(t) = d\} \quad (3)$$

if there is no sticking phase at $t = 0$.

Two types of closing contacts can occur: contacts with non-zero pre-impact velocity, commonly referred to as *impacts*, and contacts with zero pre-impact velocity. The second category can be divided as follows: *grazing* if the mass leaves the obstacle right after the gap closes, or *sticking* if the mass stays in contact with the obstacle for a finite time interval. Accordingly, the set \mathcal{H}_∞^0 can also be split into two subsets: \mathcal{H}_S^0 including all the initial data belonging to \mathcal{H}_∞^0 such that the solution starts by a sticking contact and \mathcal{H}_G^0 of initial data such that the solution starts by a grazing contact:

$$\mathcal{H}_\infty^0 = \mathcal{H}_S^0 \cup \mathcal{H}_G^0. \quad (4)$$

The first return time is known to be generically analytic with respect to the initial data: let $\mathbf{W}_0 \in \mathcal{H}^-$ and \mathbf{W}_1 the state at the first return to \mathcal{H} ; if $\mathbf{W}_1 \in \mathcal{H}^-$, then the FRT is analytic near \mathbf{W}_0 [2, 9]. However, if $\mathbf{W}_1 \in \mathcal{H}^0$, then there is a grazing contact and it is known that a square-root singularity appears [10].

¹See [8] for the definition of this set.

By definition of \mathcal{H}_P , which is not empty since it contains \mathcal{H}^- , there exists a time such that the orbit emanating from $W \in \mathcal{H}_P$ comes back to \mathcal{H}_P . The first return time is then well defined for all initial data, sticking phases set aside. In the present work, all numerical simulations are performed with $N = 2$ using the parameters $m_1 = m_2 = 1$ and $k_1 = k_2 = 1$; where not explicitly mentioned, sticking phases are not considered.

Near linear grazing modes features

The behavior of the first return time is investigated near the linear grazing modes. Let W_0 denote an initial data generating an orbit with a grazing contact at the first return time $T_0 = T(W_0)$. Then, the set of initial data with their first return time near T_0 is not a neighborhood of W_0 [8]. This means that, in the vicinity of W_0 , initial conditions might generate orbits with a first return time far from T_0 : as a consequence, the first return time $T(W)$ is discontinuous at W_0 . This discontinuity of the first return time is illustrated in the vicinity of $v_1(0) = 0$ for the two linear grazing modes of the considered two-dof system in Figure 3. The first return time can also be discontinuous near any grazing contacts, for instance, when $v_1(0)$ is near ≈ -0.2 which corresponds to the initial velocity $v_1(0)$ of an initial condition generates a nonlinear grazing orbit.

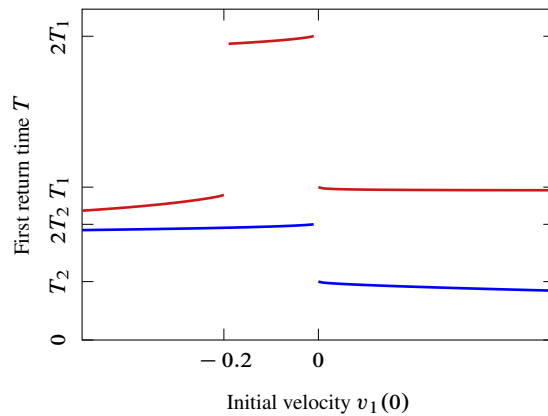


Figure 3: First return time T in the vicinity of LGM: FRT for $v_1(0) \approx v_1^{\text{LGM}_1}(0) = 0$ of the first LGM [red curves]; FRT for $v_1(0) \approx v_1^{\text{LGM}_2}(0) = 0$ of the second LGM [blue curves].

The square-root singularity is shown by zooming in the two branches of the first return time curve near the initial velocity of both linear grazing modes in Figure 3. Figure 4 shows T as a function of $v_1(0)$ near $v_1(0) = 0$.

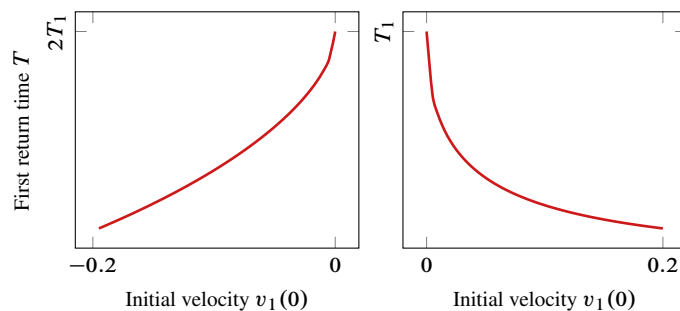


Figure 4: Square-root singularity when $v_1(0)$ varies near the initial velocity $v_1^{\text{LGM}_1}(0) = 0$ of the first LGM.

Grazing dynamics

By construction, the first return map (FRM) depends on both the trajectory and the first return time. Since the former is smooth during the free-flight, the singularity must emanate from the first return time. This singularity would a priori induce a singularity of the FRM. However, our observations suggest that the FRM smoothenes the singularity in the same way as squaring removes a square-root singularity. If this assumption does not hold, the dynamics may not be unstable as expected with the square-root singularity [8]. Overall, there are two interesting cases: near a linear grazing mode and near a periodic solution with one sticking phase-per-period (1-SPP) [7, 13]. One feature of the LGM is that the sticking phase does not occur near such a mode [8]. Hence the FRM is well defined.

Definition 3 (First return map) Suppose $W \in \mathcal{H}^- \cup \mathcal{H}_G^0$ and $T = T(W) > 0$ is the first return time to \mathcal{H}_P of the orbit emanating from W . The map which associates points in \mathcal{H}_P to their first return images to \mathcal{H}_P is called the first return

map \mathcal{F} . Formally, $\mathcal{F} : \mathcal{H}^- \cup \mathcal{H}_G^0 \rightarrow \mathcal{H}_P$ and

$$\mathcal{F}(W) = \mathbf{R}(T(W))\mathbf{S}W \tag{5}$$

where $\mathbf{S} = \text{diag}(1, \dots, 1, -1)$ is a $2N \times 2N$ diagonal matrix with last entry -1 to reflect the impact law.

FRT near a linear grazing mode

From LGM emanate multiple coexisting branches of periodic solutions with one impact-per-period (1-IPP) [9]. Also, LGM are generally expected to be unstable due to the square-root singularity [10]. The orbit of a periodic solution with one impact-per-period and with a period almost twice as much as the period of the LGM, as illustrated in Figure 5, shows clearly that the first return time is not continuous with respect to the initial data in the vicinity of a LGM.

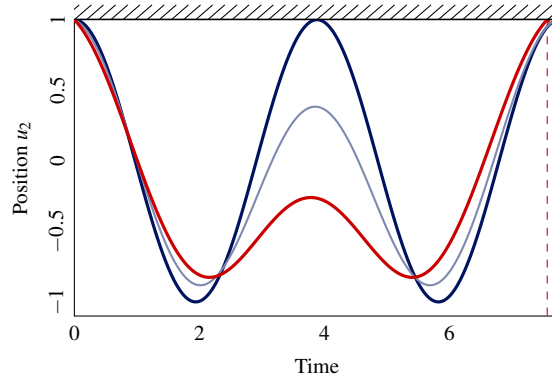


Figure 5: 1-IPP of a two-dof system near a LGM with twice its period. Within a very small change in the initial conditions, the dark blue orbit of first return time T_2 becomes the light blue orbit and then the red orbit, of first return times $\approx 2T_2$.

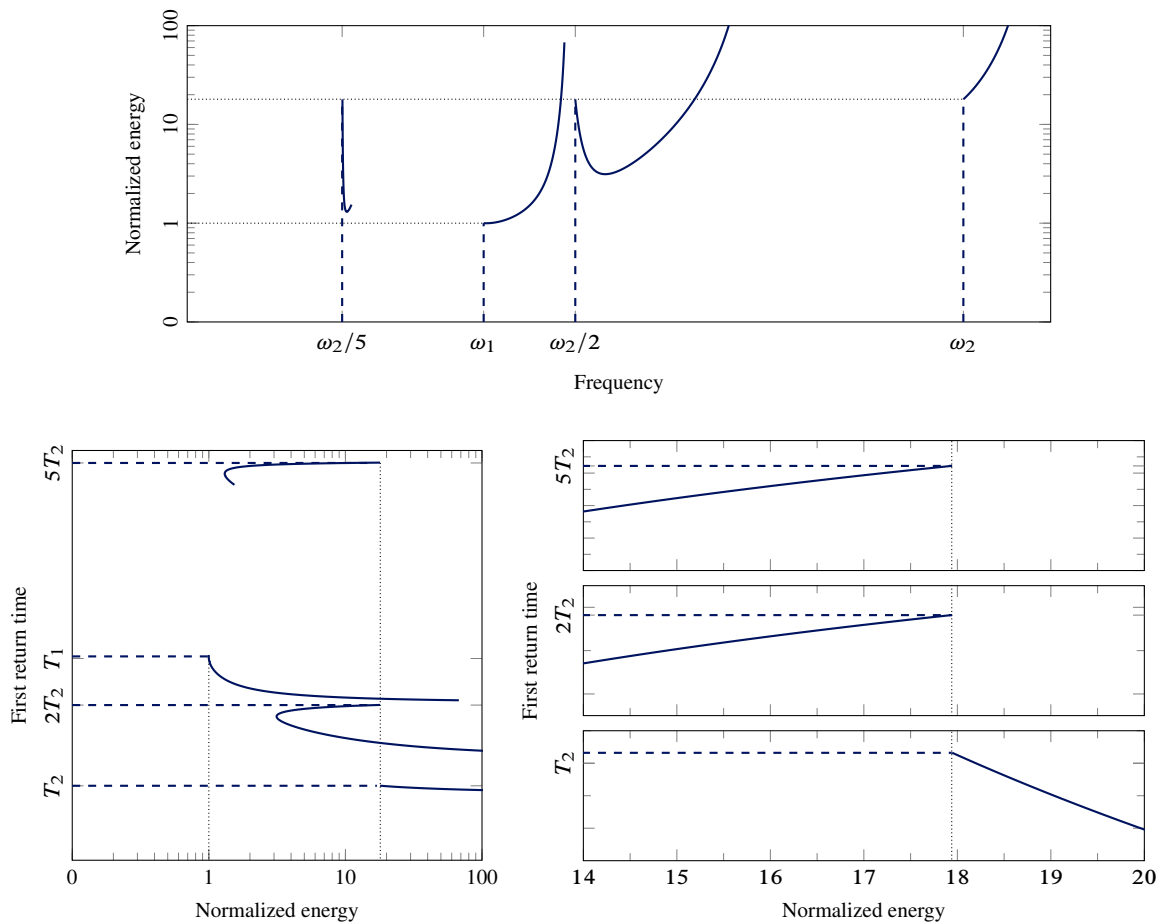


Figure 6: Top: Frequency-energy plot (FEP) of the investigated two-dof system. Bottom left: same plot represented in terms of energy-FRT. The bottom right figure is a close-up view, exhibiting the square-root singularities. The discontinuity of the FRT appears in all plots.

The frequency-energy plot in Figure 6 (top) shows the energy of several 1-IPP periodic solutions as a function of their frequency. This is a standard tool useful to vibration analysts. The vertical dashed lines corresponds to the linear modes and their harmonics. When they reach a certain level of energy, represented by the two dotted horizontal lines, they become LGM: they are still linear modes, but graze the obstacle. Then, the LGM bifurcate into various nonlinear modes represented as solid lines. The first return time of the 1-IPP is the period of the nonlinear mode and the discontinuity in frequency here corresponds to $\omega_2/1$, $\omega_2/2$, and $\omega_2/5$. The branches of a given fundamental mode and its harmonics all start at the same level of energy. If the frequency and the energy axes are reversed (Figure 6, bottom), the discontinuity of the first return time becomes obvious [9].

FRT near a periodic solution with a sticking phase

The first return map is more complicated for an orbit involving a sticking phase due to the presence of a continuum of states with zero velocity. Numerical results suggest that a cube-root singularity emerges in the first return time, as depicted in Figure 7. It can also be shown that a fourth-root singularity for the considered two-dof system may occur, as reported in [3]. More singular behaviors are expected for $N > 2$.

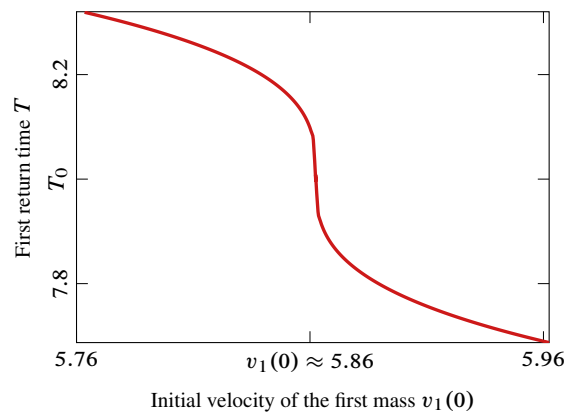


Figure 7: First return time T when a value of the initial data is changed in the vicinity of a periodic solution with one sticking phase. A cube-root singularity appears near $v_1(0) = 5.86$.

Discontinuous FRM leading to instability

The quantities in Expression (5) are either analytic or linear with respect to the initial data, except the first return time. Accordingly, a discontinuity of the first return time may imply a discontinuity of the FRM. Also, a discontinuity of the FRM at the LGM implies directly² the instability of the LGM [8].

The conservation of energy gives a condition on the discontinuity of the FRM. Moreover, the trajectories $t \mapsto \mathbf{u}(t)$ are continuous. In [1, Sec. 7, p. 254], it is shown that continuous dependence on the initial data holds for our system of interest. This means for every fixed T and $\forall \epsilon > 0$, $\exists \eta > 0$ such that if $\|\mathbf{W} - \mathbf{W}_0\| < \eta$ then $\|\mathbf{u}(t, \mathbf{W}) - \mathbf{u}(t, \mathbf{W}_0)\| < \epsilon$ for all $t \in [0; T[$. Let us consider Figure 8 representing the FRM when $v_1(0)$ is varied in the vicinity of $v_1^{\text{LGM}_j}(0) = 0$, $j = 1, 2$. It is seen that the square-root singularity is activated in almost all the components of the FRM, as proven in [8]. Also, the left and right branches of $u_1(T)$, $v_1(T)$ and $v_2(T)$ at $v_1(0) = 0$ correspond to two different continuous branches of the first return time. The square-root singularity is not activated for u_1 near both LGM [8]. Although the first return time is singular, a coefficient related to the matrix map $t \mapsto \mathbf{R}(t)$ vanishes and regularizes the singularity. Interestingly, the FRM is discontinuous for all components near $v_1(0) \approx -0.2$ as shown in Figure 8(a). However, this initial data does not correspond to a LGM.

Conclusions

In structural dynamics, it is known that orbits near grazing contacts of vibro-impact systems with a unilateral contact lead to square-root instability. In this paper, the first return map is revisited in a numerical framework to expose the theoretical results reported in [8]: square-root singularity of the first return time, activation or not of the square-root singularity in the first return map, discontinuity of the first return time and first return map. The square-root singularity and new singular behaviors such as a cube-root singularity are highlighted. The existence and the singularity of the first return time is a key step to study the first return map in the vicinity of a grazing orbit. The instability of periodic grazing orbits can be conjectured.

²As a reminder, the solution $\mathbf{u}(t) \equiv \mathbf{u}(t, \mathbf{W}_0)$ is said to be unstable if $\exists \epsilon > 0$ such that $\forall \eta > 0$, $\exists \mathbf{W}: \|\mathbf{W} - \mathbf{W}_0\| < \eta$ and $\exists t > 0$ such that $\|\mathbf{u}(t, \mathbf{W}) - \mathbf{u}(t, \mathbf{W}_0)\| > \epsilon$.

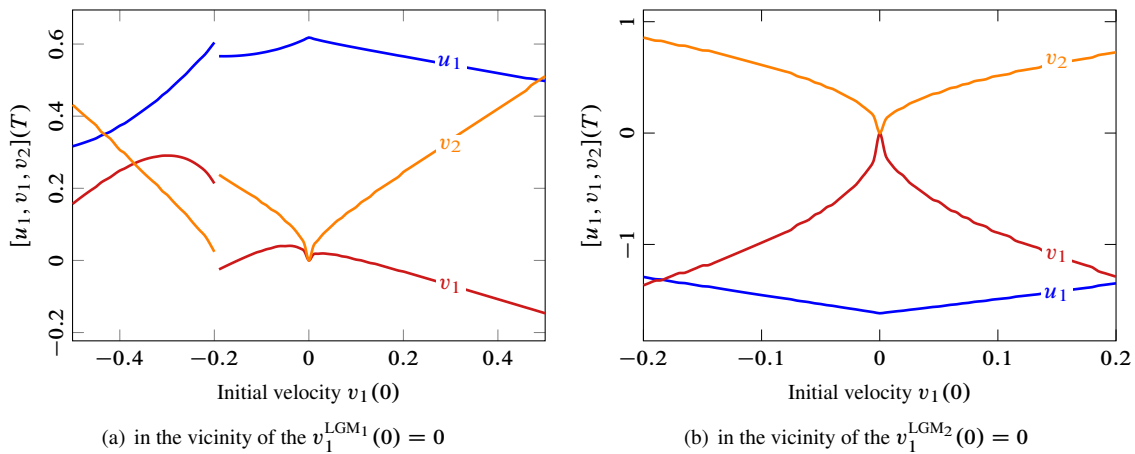


Figure 8: Cross-sections of the first return map as a function of the initial velocity $v_1(0)$.

Acknowledgment

Authors 3 and 4 would like to acknowledge the financial support of the Natural Sciences and Engineering Research Council of Canada (NSERC) and Fonds de recherche du Québec–Nature et Technologie (FQRNT).

References

- [1] Ballard P. (2000) The Dynamics of Discrete Mechanical Systems with Perfect Unilateral Constraints, *Archive for Rational Mechanics and Analysis* **154**:199-274, [[hal-00111308](#)].
- [2] di Bernardo M., Budd C., Champneys A. and Kowalczyk P. (2008) Piecewise-smooth dynamical systems: theory and applications. Springer Science & Business Media, London.
- [3] Chillingworth D. (2010) Dynamics of an impact oscillator near a degenerate graze, *Nonlinearity* **23**(11):2723-2748, [[hal-01390258](#)].
- [4] Kenneth M., Glen H., Dan O. (2009) Introduction to Hamiltonian Dynamical Systems and the N -Body Problem. Applied Mathematical Sciences, Second Edition, Springer.
- [5] Heng S. (2013) Nonlinear normal modes of impact oscillators. *Internship report*.
- [6] Kerschen G., Golinval M., Vakakis A. (2009) Nonlinear normal modes, Part I: A useful framework for the structural dynamics, *Mechanical Systems and Signal Processing* **23**:170-194, [[hal-01357931](#)].
- [7] Le Thi H., Junca S., Legrand M. (2016) Periodic solutions of a two-degree-of-freedom autonomous vibro-impact oscillator with sticking phases, *preprint* [[hal-01305719](#)].
- [8] Le Thi H., Junca S., Legrand M. (2017) First return map for a N -degree-of-freedom vibro-impact system, *in preparation*.
- [9] Legrand M., Junca S. and Heng S. (2015) Nonsmooth modal analysis of a N -degree-of-freedom system with a purely elastic impact law, *Communications in Nonlinear Science and Numerical Simulation* **45**:190-219, [[hal-01185980](#)].
- [10] Nordmark A. (2001) Existence of periodic orbits in grazing bifurcations of impacting mechanical oscillators, *Nonlinearity* **14**(6):1517-1542, [[hal-01297283](#)].
- [11] Schatzman M. (1978) A class of nonlinear differential equations of second order in time, *Nonlinear Analysis: Theory, Methods & Applications*, **2**(3):355-373, [[hal-01294058](#)].
- [12] Thorin A., Delezoide P., Legrand M. (2016) Non-smooth modal analysis of piecewise-linear impact oscillators *SIADS, in press*, [[hal-01298983](#)].
- [13] Thorin A., Delezoide P., Legrand M. (2017) Periodic solutions of n -dof autonomous vibro-impact oscillators with one lasting contact phase, [[hal-01505888](#)].
- [14] Thorin A., Legrand M., Junca S. (2015) Nonsmooth modal analysis: Investigation of a 2-dof spring-mass system subject to an elastic impact law, *Proceedings of the ASME IDETC/CIE: 11th International Conference on Multibody Systems, Nonlinear Dynamics, and Control, Boston, USA, 2015*, [[hal-01185973](#)].
- [15] Vakakis A., Manevitch L., Mikhlin Y., Pilipchuk V., Zevin A. (1996) Normal modes and localization in nonlinear systems. John Wiley & Sons.